

MIXED CONVECTION INSIDE NANOFLUID FILLED RECTANGULAR ENCLOSURES WITH MOVING BOTTOM WALL

by

Mostafa MAHMOODI

Department of Mechanical Engineering, University of Kashan, Kashan, Iran

Original scientific paper

UDC: 536.252/.253:517.96

DOI: 10.2298/TSCI101129030M

The mixed convection fluid flow and heat transfer in lid-driven rectangular enclosures filled with the Al_2O_3 -water nanofluid is investigated numerically. The left and the right vertical walls as well as the top horizontal wall of the enclosure are maintained at a constant cold temperature T_c . The bottom horizontal wall of the enclosure, which moves from left to right, is kept at a constant hot temperature T_h , with $T_h > T_c$. The governing equations written in terms of the primitive variables are solved using the finite volume method and the SIMPLER algorithm. Using the developed code, a parametric study is performed and the effects of the Richardson number, the aspect ratio of the enclosure, the volume fraction of the nanoparticles on the fluid flow, and heat transfer inside the enclosure are investigated. The results show that at low Richardson numbers, a primary counter-clockwise vortex is formed inside the enclosure. More over it is found that for the range of the Richardson number considered, 10^{-1} -10, the average Nusselt number of the hot wall, increases with increasing the volume fraction of the nanoparticles. Also it is observed that the average Nusselt number of the hot wall of tall enclosures is more than that of the shallow enclosures.

Key words: mixed convection, lid-driven, nanofluid, rectangular enclosure, finite volume method

Introduction

Mixture of nano-size particles suspended in a base fluid is named nanofluid. The nanofluid has a higher thermal conductivity in comparison with the base fluid. This higher thermal conductivity enhances the rate of heat transfer in industrial applications. Many researchers have investigated different aspects of nanofluids. Thermophysical properties of nanofluids such as thermal conductivity, thermal diffusivity, and viscosity of nanofluids have been studied by Kang *et al.* [1], Velagapudi *et al.* [2], Turgut *et al.* [3], Rudyak *et al.* [4] Murugesan *et al.* [5], and Nayak *et al.* [6].

Some works were done on the effects of nanofluids on forced convection heat transfer. Maiga *et al.* [7] studied numerically forced convection of Al_2O_3 -water and Al_2O_3 -ethylene glycol nanofluids in a straight tube of circular cross-section using the single phase model. They considered both laminar and turbulence flows. Their results for laminar flow

* Author's e-mail: mmahmoodi46@gmail.com

showed increase in rate of heat transfer and skin friction coefficient with increasing volume fraction of the nanoparticles. For turbulent flow they observed that the heat transfer coefficient increases steeply for a very short distance from the inlet section. Moreover they found that the Al_2O_3 -ethylene glycol nanofluid is more effective than to the Al_2O_3 -water nanofluid in heat transfer enhancement. Maiga *et al.* [8] analyzed numerically hydrodynamic and thermal behavior of turbulent forced convection flow of nanofluids in a circular tube. They observed an increase in heat transfer coefficient with increasing Reynolds number and the volume fraction of the nanofluids. Moreover they reported a correlation for average Nusselt number. Behzadmehr *et al.* [9] conducted a numerical study to investigate forced convection heat transfer of Cu-water nanofluid in a circular tube with a constant heat flux attached to its wall using two phase model. They observed that when the nanoparticles volume fraction equals to 1%, at a constant Reynolds number, the Nusselt number increases and the velocity profile is more uniform in comparison with the results of pure fluid. Moreover they observed decreasing skin friction coefficient by increase in Reynolds number in comparison with the pure fluid and increasing Nusselt number and heat transfer coefficient with increase in the volume fraction of the nanofluid. Santra *et al.* [10] investigated numerically effect of the Cu-water nanofluid as a cooling medium in a two-dimensional horizontal rectangular duct where top and bottom walls were isothermal. They considered the fluid Newtonian as well as non-Newtonian. They found that heat transfer enhancement is possible for both Newtonian and non-Newtonian models and increase in heat transfer is almost same for both models. Haghshenas Fard *et al.* [11] studied numerically laminar convective heat transfer of nanofluids in a circular tube under constant wall temperature condition. They used single-phase and two-phase models for prediction of temperature, flow field, and calculation of heat transfer coefficient. Their results showed that heat transfer coefficient clearly increases with increase in the volume fraction of the nanoparticles. Also they found that two-phase model shows better agreement with experimental measurements.

There are a number works about free convection of nanofluids in enclosures. First numerical study of free convection heat transfer inside rectangular cavities filled with nanofluids was done by Khanafer *et al.* [12]. They found that for the range of Grashof number considered, heat transfer increases by increase in volume fraction of the nanoparticles. Abu-Nada *et al.* [13] investigated free convection of nanofluid in horizontal concentric annuli numerically using the finite volume method. They investigated different water based nanofluids and found that for high values of Rayleigh number, nanoparticles with high thermal conductivity cause significant enhancement of heat transfer characteristics and, for intermediate values of Rayleigh number, nanoparticles with low thermal conductivity cause a reduction in heat transfer. Gumgum *et al.* [14] using the dual reciprocity boundary element method, investigated unsteady natural convective flow of nanofluids in cavities with a heat source. The results showed that the average Nusselt number increases with increase in both volume fraction of nanoparticles and Rayleigh number. It is also observed that an increase in heater length reduces the heat transfer. Sheikhzadeh *et al.* [15] conducted a numerical simulation to investigate the problem of free convection of the TiO_2 -water nanofluid in rectangular cavities differentially heated on adjacent walls. The left and the top walls of the cavities were heated and cooled; respectively, while; the cavities right and bottom walls were kept insulated. They found that by increase in the volume fraction of the nanoparticles, the mean Nusselt number of the hot wall increases for the shallow cavities; while, the reverse trend occurs for the tall cavities.

There are also a number of recent studies on mixed convection heat transfer in cavities filled with nanofluids. Tiwari *et al.* [16] used the finite volume method to investigate the flow and heat transfer in a square cavity with insulated top and bottom walls, and differentially-heated moving sidewalls. The cavity was filled with the Copper-water nanofluid. Conducting a parametric study, they investigated the effects of the Richardson number and the volume fraction of the nanoparticles on the heat transfer, and observed that when the Richardson number equals to unity, the average Nusselt number increases substantially with increase in volume fraction of the nanoparticles. Using the control volume method, Muthamilselvan *et al.* [17] investigated mixed convection heat transfer in a lid-driven rectangular enclosure filled with the Copper-water nanofluid. The enclosure's sidewalls were insulated; while, its horizontal walls were kept at constant temperatures. The top wall of the cavity was moving at a constant velocity in its own plane. They observed that both the aspect ratio of the cavity as well as the nanoparticles volume fraction affected the fluid flow and heat transfer inside the enclosure. Talebi *et al.* [18] used the finite volume method to study the mixed convection heat transfer in a lid-driven cavity filled with the Copper-water nanofluid. The vertical walls of the cavity were differentially heated; while, its top and bottom walls were kept insulated. Their results showed that, for given Reynolds and Rayleigh numbers, an increase in the volume fraction of the nanoparticles enhanced the heat transfer inside the cavity. Abu-Nada *et al.* [19] conducted a numerical investigation on mixed convection flow in an inclined square enclosure filled with Al_2O_3 -water nanofluid. The governing equations written in terms of the stream function-vorticity formulation were solved using the finite volume method. They observed significant enhancement in the heat transfer inside the cavity due to the presence of the nanoparticles. Results of a numerical study on mixed convection in a lid-driven nanofluid filled square cavity with cold side and top wall, a constant heat flux heater on the bottom wall and moving lid were reported by Mansuor *et al.* [20]. The effects of Reynolds number, type of nanofluids, size and location of the heater and the volume fraction of the nanoparticles were considered in their study. Their results showed that the rate of heat transfer increases with increase in the length of the heater, Reynolds number and the nanoparticles volume fraction. Moreover they found that maximum and minimum rate of heat transfer is obtained by adding the Al_2O_3 and TiO_2 nanoparticles to the base fluid, respectively. In a very recent study, Arefmanesh *et al.* [21] have investigated mixed convection of Al_2O_3 -water nanofluid in a cavity with insulated side walls, wavy hot bottom wall and moving cold top wall. They observed that distributions of the local Nusselt number along the wavy hot wall closely follow the pattern of the wall's geometry for different Richardson numbers and the nanoparticles volume fractions considered.

In the all above mentioned numerical studies on mixed convection in lid-driven enclosures to estimate the effective dynamic viscosity of nanofluid the Brinkman formula [22] is used. In a numerical study Abu-Nada *et al.* [23] investigated the effects of different models of viscosity of Al_2O_3 -water and CuO -water nanofluids on numerical simulation of natural convection heat transfer in rectangular enclosures. They observed that the Brinkman model does not estimate the effective dynamic viscosity of nanofluid truly. In this study, the mixed convection fluid flow and heat transfer in rectangular enclosures filled with the Al_2O_3 -water nanofluid is simulated numerically using the finite volume method. The left and the right vertical walls as well as the top horizontal wall of the enclosure are kept at a constant temperature T_c . The enclosure's bottom wall, which moves in its own plane from left to right with a constant speed, is maintained at a constant temperature T_h which is higher than T_c . This problem may finds application for design of heat exchangers using nanofluids. On the basis of

the results of Abu-Nada *et al.* [23], contrary to the previous numerical studies on mixed convection in enclosures, the Maiga *et al.* correlation [7] based on the experimental results of Wang *et al.* [24] is used to estimate effective dynamic viscosity of Al_2O_3 -water nanofluid. A parametric study is performed, and the effects of the Richardson number, aspect ratio of the enclosure, and the volume fraction of the nanoparticles on the fluid flow and heat transfer inside the enclosure are investigated.

Mathematical modeling

A schematic view of the enclosure considered in the present study is shown in fig 1. The height and the width of the enclosure are denoted by H and W , respectively. The aspect ratio is defined as $AR = H/W$. The length of the enclosure perpendicular to the plane of the figure is assumed to be long hence, the problem is considered two-dimensional. The left and the right, as well as, the top wall of the enclosure are maintained at a constant temperature T_c . The enclosure's bottom wall, which moves in its own plane from left to right, is kept at a constant temperature T_h , with $T_h > T_c$. The enclosure is filled with a nanofluid composed of a mixture of water and Al_2O_3 spherical nanoparticles. The nanofluid is assumed to be incompressible, and the flow is considered to be laminar. The nanoparticles are presumed to be in thermal equilibrium with the water. Moreover, there is no slip between the nanoparticles and the base fluid. The thermophysical properties of the fluid phase and the nanoparticles at $T = 25^\circ$ are presented in tab. 1. The Prandtl number of the fluid phase is equal to $Pr = 6.8$. The nanofluid properties are assumed to be constant with the exception of the density which varies according to the Boussinesq approximation [25].

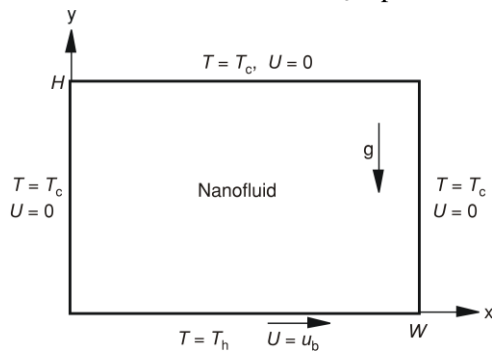


Figure 1. Schematic view of the rectangular enclosure considered in the present study

Moreover, there is no slip between the nanoparticles and the base fluid. The thermophysical properties of the fluid phase and the nanoparticles at $T = 25^\circ$ are presented in tab. 1. The Prandtl number of the fluid phase is equal to $Pr = 6.8$. The nanofluid properties are assumed to be constant with the exception of the density which varies according to the Boussinesq approximation [25].

Table 1. Thermophysical properties of the base fluid and the Al_2O_3 nanoparticles at $T = 25^\circ$

	C_p [$\text{Jkg}^{-1}\text{K}^{-1}$]	ρ [kgm^{-3}]	k [$\text{Wm}^{-1}\text{K}^{-1}$]	$\beta \cdot 10^{-5}$ [K^{-1}]
Fluid phase	4179	997.1	0.613	21
Al_2O_3	765	3970	25	0.85

In this section, the equations which govern the mixed convection fluid flow and heat transfer inside the enclosure are presented in a dimensionless form. The following dimensionless variables are introduced for this purpose:

$$X = \frac{x}{W}, \quad Y = \frac{y}{H}, \quad U = \frac{u}{u_b}, \quad V = \frac{v}{u_b}, \quad \theta = \frac{T - T_c}{T_h - T_c}, \quad P = \frac{P}{\rho_{nf} u_b^2} \quad (1)$$

Employing the above dimensionless variables, the continuity, momentum, and energy equations for the nanofluid in the enclosure, under steady-state conditions,

incorporating the natural convection through the Boussinesq approximation in the y-momentum equation, are written as:

$$\frac{\partial U}{\partial X} + \frac{\partial V}{\partial Y} = 0 \quad (2)$$

$$U \frac{\partial U}{\partial X} + V \frac{\partial U}{\partial Y} = -\frac{\partial P}{\partial X} + \frac{1}{\text{Re}} \frac{\mu_{\text{eff}}}{\nu_f \rho_{\text{nf}}} \left(\frac{\partial^2 U}{\partial X^2} + \frac{\partial^2 U}{\partial Y^2} \right) \quad (3)$$

$$U \frac{\partial V}{\partial X} + V \frac{\partial V}{\partial Y} = -\frac{\partial P}{\partial Y} + \frac{1}{\text{Re}} \frac{\mu_{\text{eff}}}{\nu_f \rho_{\text{nf}}} \left(\frac{\partial^2 V}{\partial X^2} + \frac{\partial^2 V}{\partial Y^2} \right) + \frac{(\rho\beta)_{\text{nf}}}{\rho_{\text{nf}} \beta_f} \text{Ri} \theta \quad (4)$$

$$U \frac{\partial \theta}{\partial X} + V \frac{\partial \theta}{\partial Y} = \frac{\alpha_{\text{nf}}}{\alpha_f} \frac{1}{\text{PrRe}} \left(\frac{\partial^2 \theta}{\partial X^2} + \frac{\partial^2 \theta}{\partial Y^2} \right) \quad (5)$$

Reynolds number, Re, Richardson number, Ri, and the Prandtl number, Pr, are defined as:

$$\text{Re} = \frac{u_b W}{\nu_f}, \quad \text{Ri} = \frac{g \beta_f (T_h - T_c) W}{u_b^2}, \quad \text{Pr} = \frac{\nu_f}{\alpha_f} \quad (6)$$

Moreover, $\text{Ri} = \text{Gr}/\text{Re}^2$ where the Grashof number Gr, is defined as:

$$\text{Gr} = \frac{g \beta_f (T_h - T_c) W^3}{\nu_f^2} \quad (7)$$

The boundary conditions for eqs. (2–5) are:

$$U = V = 0, \quad \theta = 0 \quad \text{at left, right, and top walls} \quad (8a)$$

$$U = 1, \quad V = 0, \quad \theta = 1 \quad \text{at bottom wall} \quad (8b)$$

The effective dynamic viscosity of the nanofluid can be obtained from various formulas available in the literature. In this study the correlation proposed by Maiga *et al.* [7] based on the experimental results of Wang *et al.* [24] according to the following is used to estimate the viscosity of the Al₂O₃-water nanofluid:

$$\mu_{\text{eff}} = \mu_f (1 + 7.3\phi + 123\phi^2) \quad (10)$$

The density, ρ_{nf} , the heat capacity, $(\rho c_p)_{\text{nf}}$, and the thermal expansion coefficient, $(\rho\beta)_{\text{nf}}$, of the nanofluid are obtained from the formulas:

$$\rho_{\text{nf}} = (1 - \phi)\rho_f + \phi\rho_s \quad (11)$$

$$(\rho c_p)_{\text{nf}} = (1 - \phi)(\rho c_p)_f + \phi(\rho c_p)_s \quad (12)$$

$$(\rho\beta)_{\text{nf}} = (1 - \phi)(\rho\beta)_f + \phi(\rho\beta)_s \quad (13)$$

The effective thermal conductivity of the nanofluid, k_{eff} , for spherical nanoparticles is evaluated from the Maxwell model [26]:

$$\frac{k_{\text{eff}}}{k_f} = \frac{k_s + 2k_f - 2\phi(k_f - k_s)}{k_s + 2k_f - \phi(k_f - k_s)} \quad (14)$$

The thermal diffusivity of the nanofluid is expressed as:

$$\alpha_{\text{nf}} = \frac{k_{\text{eff}}}{(\rho c_p)_{\text{nf}}} \quad (15)$$

The Nusselt number based on the width of the enclosure is evaluated from the relation:

$$\text{Nu} = \frac{h_{\text{nf}} W}{k_f} \quad (16)$$

The heat transfer coefficient, h_{nf} , is obtained from:

$$h_{\text{nf}} = \frac{q}{A(T_h - T_c)} \quad (17)$$

The wall heat flux per unit area, q , can be written as:

$$q = -k_{\text{nf}} \frac{A(T_h - T_c)}{W} \left. \frac{\partial \theta}{\partial Y} \right|_{\text{wall}} \quad (18)$$

Substituting eqs. (15) and (16) in eq. (14) yields the following relation for the Nusselt number:

$$\text{Nu}(X) = -\frac{k_{\text{nf}}}{k_f} \left. \frac{\partial \theta}{\partial Y} \right|_{\text{wall}} \quad (19)$$

The averaged Nusselt number of the hot wall can be obtained by integrating the local Nusselt number along the wall as:

$$\overline{\text{Nu}} = \int_0^1 \text{Nu}(X) dX \quad (20)$$

Numerical approach

The governing mass, momentum, and energy equations written in terms of the primitive variables are discretized using the finite volume approach and the coupling between velocity and pressure is done using the SIMPLER algorithm [27]. The diffusion terms are discretized using a second-order central difference scheme; while, an upwind scheme is employed to discretize the convective terms. The set of discretized equations are solved iteratively yielding values of the velocity, pressure, and temperature at the nodal points. An under-relaxation scheme is employed to obtain converged solutions.

In order to validate the proposed numerical scheme, the problem of mixed convection fluid flow and heat transfer in an air filled differentially-heated square enclosure with insulated horizontal wall, cold and hot moving upward left and right walls, according to the geometry considered in work of Oztop *et al.* [28] is analyzed using the presented code, and the results are compared with existing results in the literatures.

Table 2 shows the average Nusselt number of the hot sidewall for different Richardson numbers obtained by the present simulation. The results of Oztop *et al.* [28] for the same problem are also shown in this table. As can be seen from this table, very good agreements exist between the two results.

In order to determine a proper grid for the numerical simulation, a grid independence study is undertaken for the mixed convection heat transfer in the enclosure shown in fig. 1 with $AR = 1$ ($H = W$) filled with pure fluid at $Ri = 0.01$. Six different uniform grids, namely, 21×21 , 41×41 , 61×61 , 81×81 , 101×101 and 121×121 are employed for the numerical simulation. The X -component of the velocity along the vertical centerline of the enclosure and the Y -component of the velocity along the horizontal centerline of the enclosure for these grids are shown in figs. 2(a) and 2(b), respectively. Based on these results, an 81×81 uniform grid is used for all the results to be presented in the following.

Table 2. Comparison of the present results for the average Nusselt number of the heated wall with the results of Oztop *et al.* [28]

	Present study	Oztop <i>et al.</i> [28]
Ri = 100	1.051	1.048
Ri = 10	0.965	0.961
Ri = 1	1.928	1.921
Ri = 0.1	3.411	3.406
Ri = 0.01	6.382	6.376

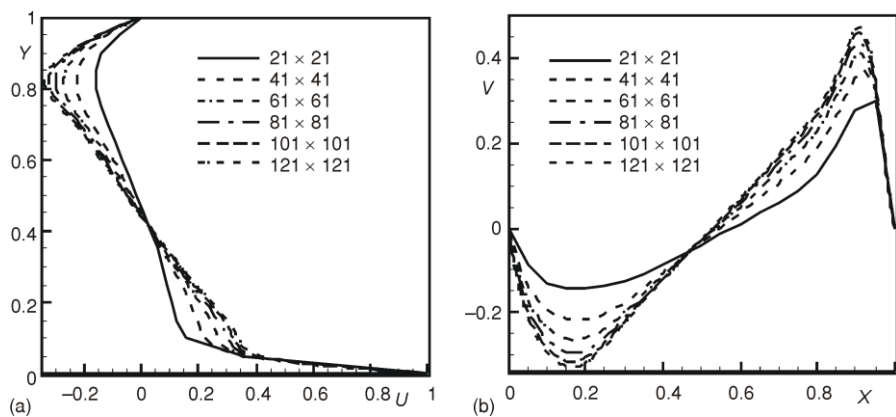


Figure 2. Velocity components along the square enclosure centerlines for different uniform grids; (a) $U(0.5, Y)$, $0 \leq Y \leq 1$, (b) $V(X, 0.5)$, $0 \leq X \leq 1$

Results and discussion

Having validated the numerical procedure via solving the test case, the code is employed to investigate the mixed convection fluid flow and heat transfer inside the rectangular enclosures filled nanofluid. The results are presented for $Gr = 10^4$, a range of Ri

from 0.1 to 10, three different aspect ratio of enclosure, namely, 0.5, 1, and 2, and four volume fractions of the nanofluids, namely, 0, 0.03, 0.06, and 0.1.

Figure 3 show the streamlines and the isotherms inside the enclosure with $AR = 1$ for various Richardson numbers, and different volume fractions of the nanoparticles. For $Ri = 0.1$, the flow is established by the moving bottom lid. A large, counterclockwise primary eddy is formed inside the enclosure as a result of the nanofluid moving next to the bottom wall. A small, clockwise eddy referred to as the DSE (downstream eddy) develops in the top right corner of the enclosure as a result of the stagnation pressure and frictional losses. Another smaller, clockwise eddy called the USE (upstream eddy) exists at the top left corner of the enclosure which is due to the negative pressure gradient generated by the primary circulating nanofluid as it deflects downward over the left vertical wall of the enclosure. As it can be seen from the figure, with increase of Richardson number, for a constant volume fraction of the nanoparticles, the effect of the natural convection on the fluid flow and heat transfer inside the enclosure intensifies. Consequently, the nanofluid adjacent to the cold right wall of the enclosure moves downward, and enlarges the DSE causing it to occupy a major portion of the enclosure for high Richardson numbers. The primary eddy diminishes as a result of the increasing the size of the DSE. Moreover, due to the nanofluid moving downward next to the cold left wall of the enclosure, the USE diminishes in size, and finally disappears when the Richardson number increases. It is observable from the figure that the size and strength of the DSE diminish when the volume fraction of the nanoparticles increases

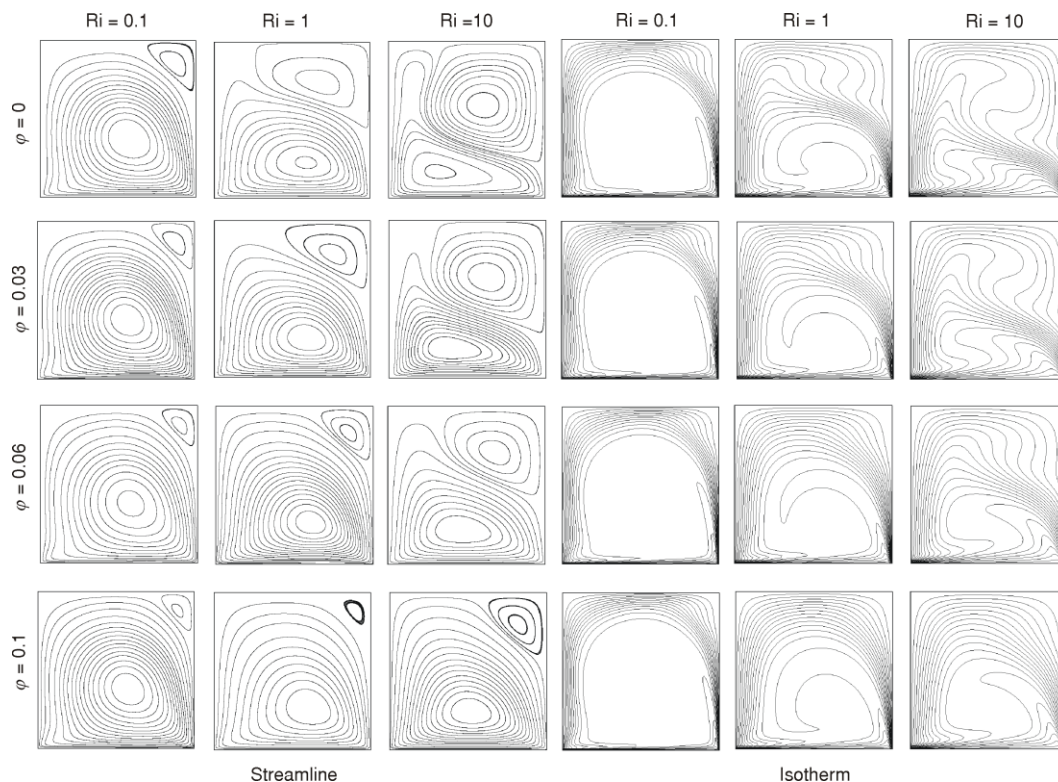


Figure 3. Streamlines and isotherms for enclosure with $AR = 1$

for a constant Richardson number. This effect, which can be clearly seen for $Ri = 1$, is due to suppression of the natural convection inside the enclosure with increase in the volume fraction of the nanoparticles and the resulting increase in the effective viscosity of the nanofluid. Moreover, the primary eddy grows as a result of DSE being diminished. Also, it is observed from the figure that for low Richardson number ($Ri = 0.1$), the flow field established by the moving bottom wall, and, as such, is relatively insensitive to changing the volume fraction of the nanoparticles. From the isotherms shown in fig. 3, the following phenomena are observable. At $Ri = 0.1$, the existence of distinct thermal boundary layers adjacent to the enclosure's walls shows a forced convection-dominated regime. The core region of the enclosure is nearly isothermal.

With increasing the Richardson number, for a constant volume fraction of the nanoparticles, the DSE enlarges, and the thermal boundary layers thicken. Consequently, the isotherms get more evenly distribution inside the enclosure. On the other hand, at $Ri = 10$, the fluid flow inside the enclosure dominated by the natural convection. This can be clearly seen from the distribution of the isotherms in the figure.

Streamlines and isotherms inside tall enclosures ($AR = 2$) with respect to the Richardson number and volume fraction of the nanoparticles are shown in fig. 4. Similar to the case of square enclosure ($AR = 1$) for $Ri = 0.1$, a primary clockwise eddy is formed inside the cavity as a result of the nanofluid moving next to the bottom wall. The difference is that for tall enclosure, the primary eddy occupies lower half of the enclosure while the upper half of the enclosure is occupied by DSE. When the Richardson number increases, while the volume fraction of the nanoparticles is constant, the primary eddy diminishes in size and its core moves downward. Moreover, when the Richardson number increases, the primary eddy enlarges to the top left corner of the enclosure and its size in right half of the enclosure, diminishes. It causes the core of the DSE to move downward and its size to diminish in horizontal direction. At $Ri = 0.1$, the flow field established by the moving bottom wall, and, is relatively insensitive to variation of the volume fraction of the nanoparticles. At moderate Richardson number ($Ri = 1$), that natural and forced convection are comparable, due to the suppression of the natural convection inside the enclosure with increase in the effective viscosity of the nanofluid, the size of the DSE, which is affected by natural convection, diminishes. A similar trend to $Ri = 1$, is observed from results of $Ri = 10$. From the isotherms for tall enclosure, the following phenomena are observable. Forced convection-dominated regime for $Ri = 0.1$, is found from distinct thermal boundary layers adjacent to the walls of the enclosure. Different temperature distributions in upper half of the enclosure at this Richardson number are results of natural convection and existence of DSE in this region. With increasing the Richardson number, natural convection become stronger, and the thermal boundary layers thicken.

Figure 5 shows streamlines and isotherms inside shallow enclosure with $AR = 0.5$ for different Richardson numbers and different volume fraction of the nanoparticles. As shown in the figure at $Ri = 0.1$, the primary eddy which was observed for tall and square enclosures, occupies major portion of the enclosure. The size of the DSE is bigger than that for enclosures with different aspect ratio at this Richardson number. At $Ri = 0.1$ by increase in the volume fraction of the nanoparticles and the effective dynamic viscosity of the nanofluid, the size of the DSE decreases and finally at $\phi = 0.1$, it disappears. With increase in Richardson number, for a constant volume fraction of the nanoparticles, the effects of natural convection is intensified, that results in enhancement of DSE. For $Ri = 1$, and 10, by increase in the effective viscosity of the nanofluids via increase in the nanoparticles volume fraction,

the DSE, which is motivated by the natural convection, decreases in size and strength. For shallow enclosures, the USE is not developed for all range of Richardson number and volume fraction of the nanoparticles considered. The observed phenomena about isotherms for tall and square enclosures are valid for shallow enclosures.

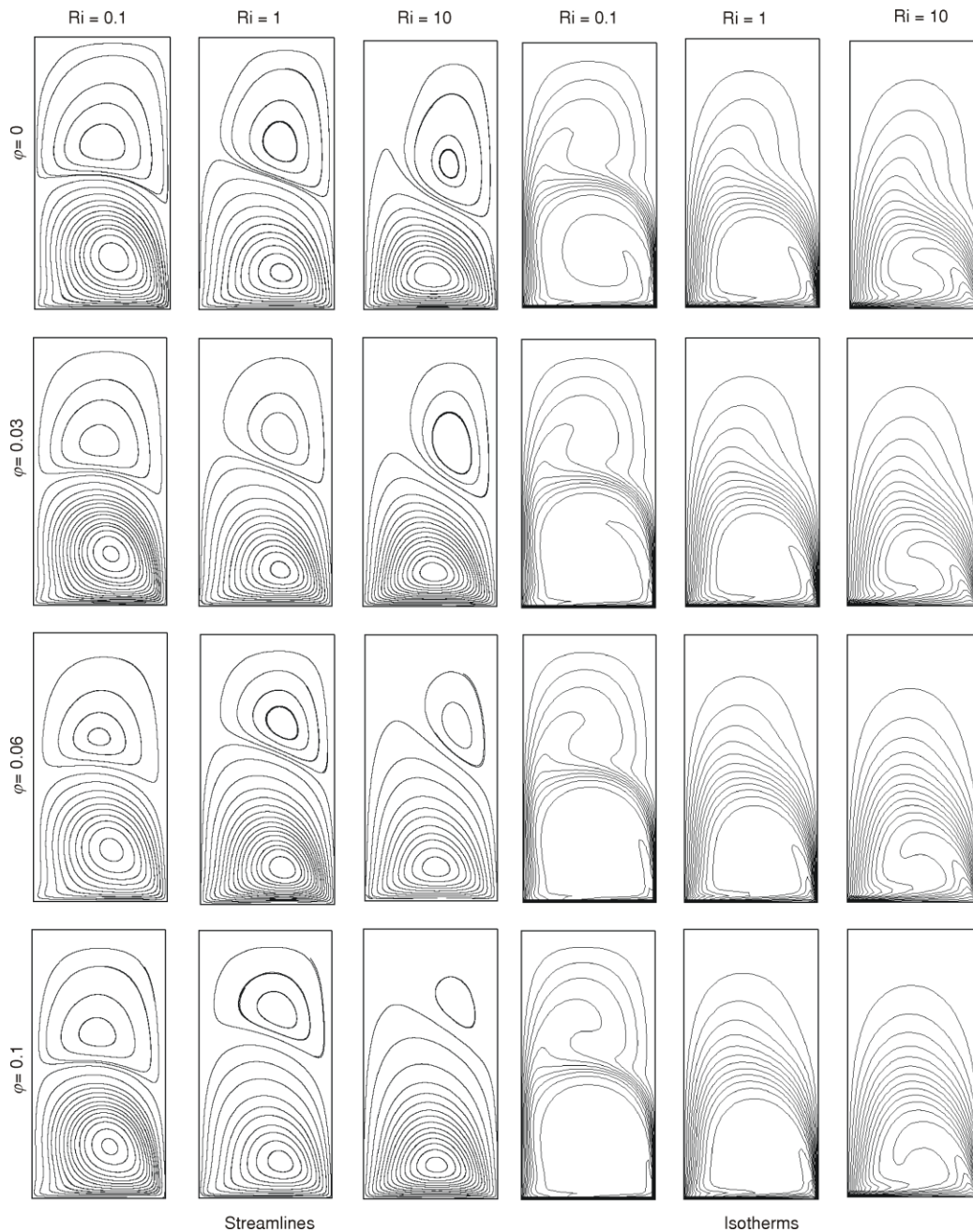


Figure 4. Streamlines and isotherms for tall enclosure with $AR = 2$

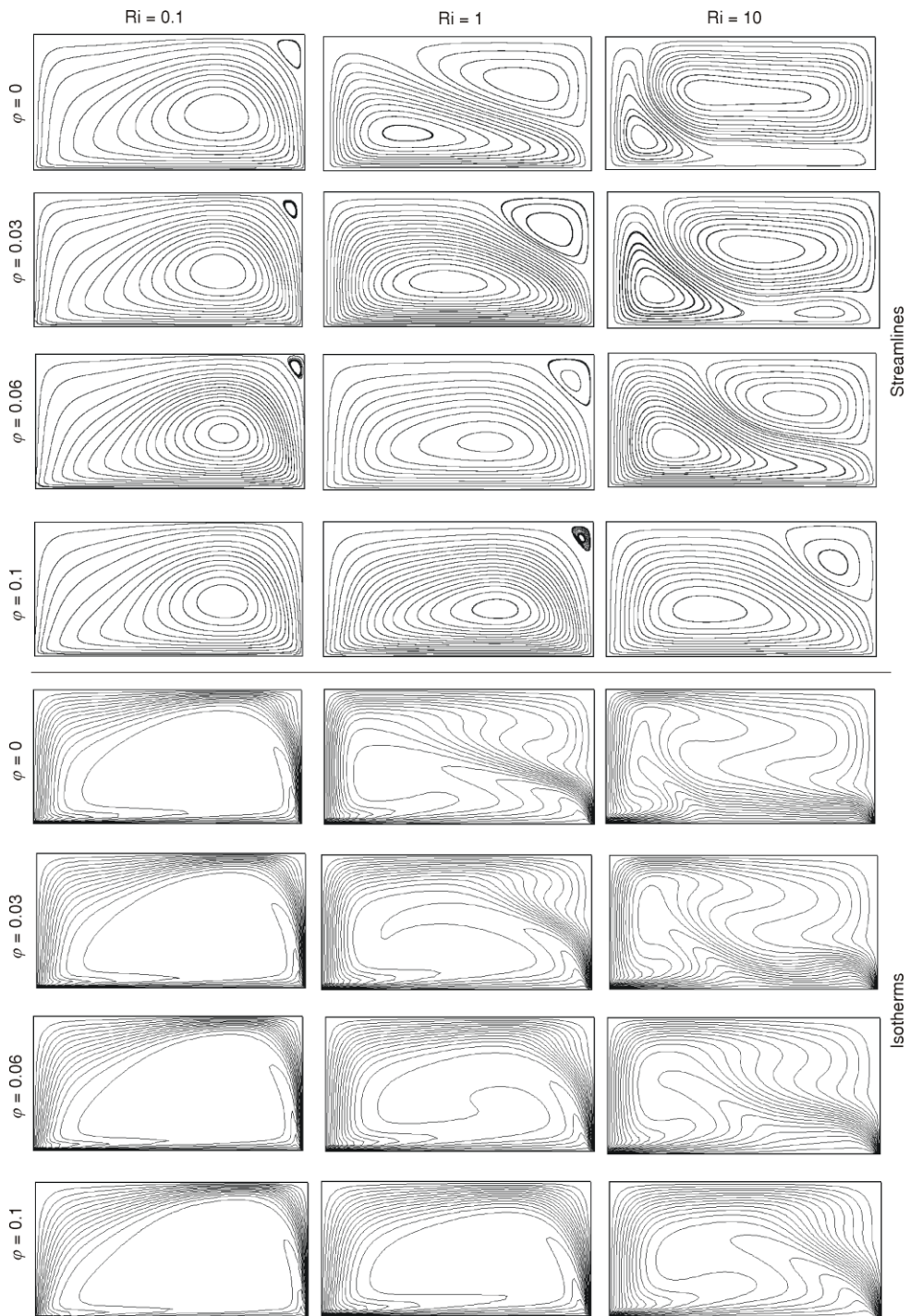


Figure 5. Streamlines and isotherms for shallow enclosure with $AR = 0$

Figure 6 shows variation of average Nusselt number of the hot wall of the enclosure with the volume fraction of the nanoparticles for different Richardson numbers and different aspect ratios. As it is observed from the figure, a difference exists between average Nusselt numbers of pure fluid and nanofluid. Also the average Nusselt number increases by increase

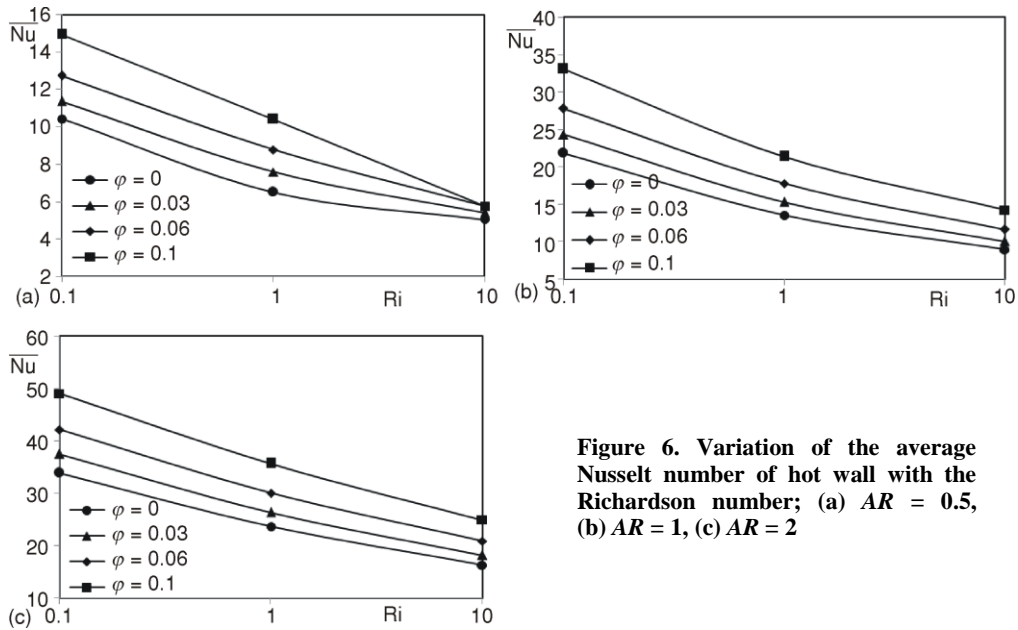


Figure 6. Variation of the average Nusselt number of hot wall with the Richardson number; (a) AR = 0.5, (b) AR = 1, (c) AR = 2

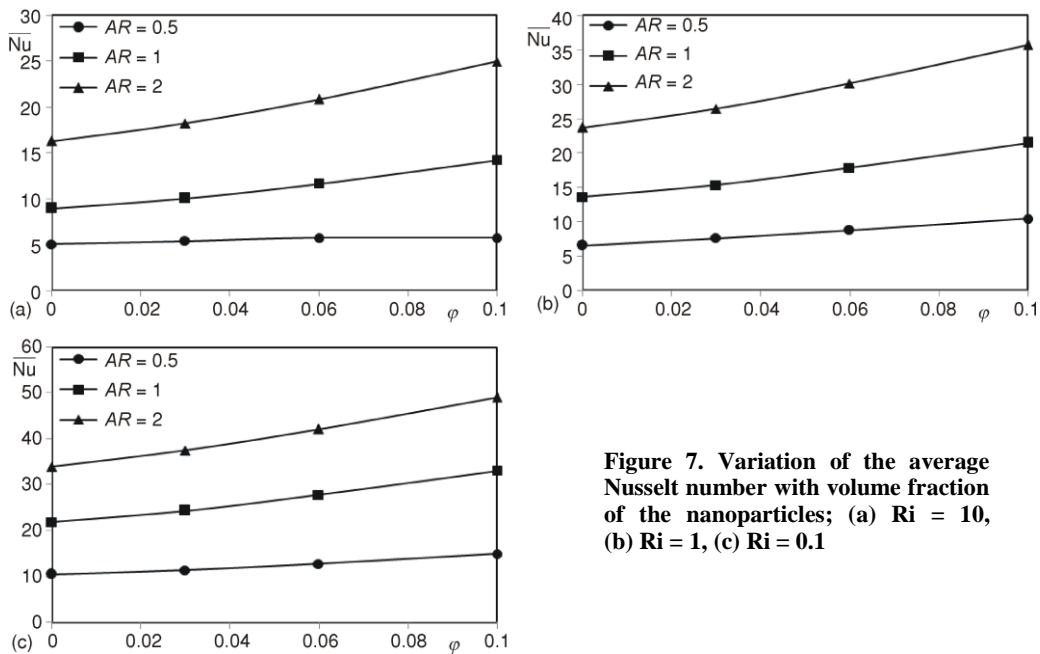


Figure 7. Variation of the average Nusselt number with volume fraction of the nanoparticles; (a) Ri = 10, (b) Ri = 1, (c) Ri = 0.1

in the volume fraction of the nanoparticles. It is motivated by higher thermal conductivity of nanofluid than that of the base fluid. Also, the difference between the average Nusselt numbers of pure fluid and nanofluid increases with decrease in the Richardson number. The decrease of Richardson number also increases the heat transfer rate and hence average Nusselt number. This is because of higher velocity of the cavity wall and therefore higher shear force achieved at lower Richardson number. These observations are valid for all aspect ratios considered.

For better comparison, variation of the average Nusselt numbers with aspect ratios and volume fraction of the nanoparticles is shown in fig. 7 for each Richardson number separately. This figure shows a linear variation of the average Nusselt number with the volume fraction of the nanoparticles. Also it can be clearly seen from the figure that the rate of heat transfer increases when the volume fraction of the nanoparticles increases. From results at all Richardson numbers it evident that the average Nusselt number increases when the aspect ratio of the enclosure increases. It means that maximum rate of heat transfer occurs for tall enclosure while, its minimum occurs for shallow enclosure. Furthermore, it is found that rate of increase in the average Nusselt number with increase in the volume fraction of the nanoparticles, increases when the aspect ratio of the enclosure increases.

Conclusions

The mixed convection fluid flow and heat transfer in rectangular enclosures filled with Al_2O_3 -water nanofluid was studied numerically using the finite volume method. The forced convective flow within the enclosure is attained by a moving bottom wall, while the natural convective effect is obtained by subjecting the bottom wall to a higher temperature than those of the other walls which are kept at the same temperature. The effects of the Richardson number, the volume fraction of the nanoparticles and aspect ratio of the enclosure on the flow field, and heat transfer inside the enclosure were investigated. It is found that for all range of aspect ratios considered, at low Richardson number ($\text{Ri} = 0.1$) a primary counter clockwise vortex was formed inside the enclosure that its size decreased by increase in the Richardson number and domination of natural convection. Also it was observed that, for all aspect ratios considered, for the Richardson numbers between 0.1 and 10, the average Nusselt number increased by increasing the volume fraction of the nanoparticles. This phenomenon was more remarkable at low Richardson numbers. Moreover, it was found that maximum average Nusselt number occurred for tall enclosure and its minimum is found for shallow enclosure. Finally it was found that rate of increase in the average Nusselt number with volume fraction of the nanoparticles, increased when the aspect ratio of the enclosure increased.

Nomenclature

AR	– aspect ratio of enclosure	P	– dimensionless pressure
c_p	– specific heat, [$\text{Jkg}^{-1}\text{K}^{-1}$]	Pr	– Prandtl number, [–]
Gr	– Grashof number, [–]	p	– pressure, [Nm^{-2}]
g	– gravitational acceleration, [ms^{-2}]	q	– heat flux per unit area, [Wm^{-2}]
H	– enclosure height, [m]	Re	– Reynolds number, [–]
h	– heat transfer coefficient, [$\text{Wm}^{-2}\text{K}^{-1}$]	Ri	– Richardson number, [–]
k	– thermal conductivity, [$\text{Wm}^{-1}\text{K}^{-1}$]	T	– temperature, [K]
Nu	– Nusselt number, [–]	U, V	– dimensionless velocity components

u, v	– velocity components, [ms^{-1}]	ρ	– density, [kgm^{-3}]
u_b	– lid-velocity	ϕ	– volume fraction of the nanoparticles
X, Y	– dimensionless Cartesian co-ordinates	Subscripts	
x, y	– Cartesian co-ordinates, [m]	avg	– average
Greek symbols		c	– cold
α	– thermal diffusivity, [m^2s^{-1}]	eff	– effective
β	– thermal expansion coefficient, [K^{-1}]	f	– fluid
θ	– dimensionless temperature	h	– hot
μ	– dynamic viscosity, [$\text{kgm}^{-1}\text{s}^{-1}$]	nf	– nanofluid
ν	– kinematic viscosity, [m^2s^{-1}]	s	– solid particles

References

- [1] Kang, H. U., Kim, S. H., Oh, J. M., Estimation of Thermal Conductivity of Nanofluid using Experimental Effective Particle Volume, *Exp. Heat Transfer*, 19 (2006), 3, pp. 181-191
- [2] Velagapudi, V., Konijeti, R. K., Aduru, C. S. K., Empirical Correlation to Predict Thermophysical and Heat Transfer Characteristics of Nanofluids, *Thermal Science*, 12 (2008), 2, pp. 27-37
- [3] Turgut, A., *et al.*, Thermal Conductivity and Viscosity Measurements of Water-Based TiO_2 Nanofluids, *Int. J. Thermophys*, 30 (2009), 4, pp. 1213-1226
- [4] Rudyak, V. Y., Belkin, A. A., Tomilina, E. A., On the Thermal Conductivity of Nanofluids, *Technical Physics Letters*, 36 (2010), 7, pp. 660-662
- [5] Murugesan, C., Sivan, S., Limits for Thermal Conductivity of Nanofluids, *Thermal Science*, 14 (2010), 1, pp. 65-71
- [6] Nayak, A. K., Singh, R. K., Kulkarni, P. P., Measurement of Volumetric Thermal Expansion Coefficient of Various Nanofluids, *Technical Physics Letters*, 36 (2010), 8, pp. 696-698
- [7] Maiga, S. E. B., *et al.*, Heat Transfer Behaviors of Nanofluids in a Uniformly Heated Tube, *Superlattices and Microstructures*, 35 (2004), 3-6, pp. 543-557
- [8] Maiga, S. B., Nguyen, C. T., Heat Transfer Enhancement in Turbulent Tube Flow Using Al_2O_3 Nanoparticles Suspension, *Int. J. Num. Method Heat Fluid Flow*, 16 (2006), 3, pp. 275-292
- [9] Behzadmehr, A., Saffar-Avval, M., Galanis, N., Prediction of Turbulence Forced Convection of a Nanofluid in a Tube with Uniform Heat Flux Using Two Phase Approach, *Int. J. Heat Fluid Flow*, 28 (2007), 2, pp. 211-219
- [10] Santra, A. P., Sen, S., Chakraborty, N., Study of Heat Transfer Due to Laminar Flow of Copper-Water Nanofluid through Two Isothermally Heated Parallel Plate, *Int. J. Thermal Sci.*, 48 (2009), 2, pp. 391-400
- [11] Haghshenas Fard, M., Nasr Esfahany, M., Talaie, M. R., Numerical Study of Convective Heat Transfer of Nanofluids in a Circular Tube Two-Phase Model Versus Single-Phase Model, *Int. Comm. Heat Mass Trans.*, 37 (2010), 1, pp. 91-97
- [12] Khanafer, K., Vafai, K., Lightstone, M., Buoyancy-Driven Heat Transfer Enhancement in a Two-Dimensional Enclosure Utilizing Nanofluid, *Int. J. Heat Mass Tran.*, 46 (2003), 19, pp. 3639-3653
- [13] Abu-Nada, E., Masoud, Z., Hijazi, A., Natural Convection Heat Transfer Enhancement in Horizontal Concentric Annuli Using Nanofluids, *Int. Comm. Heat Mass Trans.*, 35 (2008), 5, pp. 657-665
- [14] Gumguma, S., Tezer-Sezgin, M., DRBEM Solution of Natural Convection Flow of Nanofluids with a Heat Source, *Engineering Analysis with Boundary Elements*, 34 (2010), 8, pp. 727-737
- [15] Sheikhzadeh, G. A., Arefmanesh, A., Mahmoodi, M., Numerical Study of Natural Convection in a Differentially-Heated Rectangular Cavity Filled with TiO_2 -Water Nanofluid, *Journal of Nano Research*, 13 (2011), pp. 75-80
- [16] Tiwari, R. K., Das, M. K., Heat Transfer Augmentation in a Two-Sided Lid-Driven Differentially Heated Square Cavity Utilizing Nanofluids, *Int. J. Heat Mass Tran.*, 50 (2007), 9-10, pp. 2002-2018
- [17] Muthamilselvan, M., Kandaswamy, P., Lee, J., Heat Transfer Enhancement of Copper-Water Nanofluids in a Lid-Driven Enclosure, *Commun Nonlinear Sci Numer Simulat.*, 15 (2010), 6, pp. 1501-1510

- [18] Talebi, F., Mahmoudi, A. H., Shahi, M., Numerical Study of Mixed Convection Flows in a Square Lid-Driven Cavity Utilizing Nanofluid, *Int. Comm. Heat Mass Trans.*, 37 (2010), 1, pp. 79-90
- [19] Abu-Nada, E., Chamkha, A. J., Mixed Convection Flow in a Lid-Driven Square Enclosure Filled with a Nanofluid, *European Journal of Mechanic B/Fluids*, 29 (2010), 6, pp. 472-482
- [20] Mansour, M. A., *et al.*, Numerical Simulation of Mixed Convection Flows in a Square Lid-Driven Cavity Partially Heated from below Using Nanofluid, *International Communications in Heat and Mass Transfer*, 37 (2010), 10, pp. 1504-1512
- [21] Arefmanesh, A., Najafi, M., Nikfar, M., Meshless Local Petrov-Galerkin Simulation of Buoyancy-Driven Fluid Flow and Heat Transfer in a Cavity with Wavy Side Walls, *Computer Modeling in Engineering & Sciences*, 62 (2010), 2, pp. 113-149
- [22] Brinkman, H. C., The Viscosity of Concentrated Suspensions and Solutions, *J. Chem. Phys.*, 20 (1952), 4, pp. 571-581
- [23] Abu-Nada, E., *et al.*, Effect of Nanofluid Variable Properties on Natural Convection in Enclosures, *Int. J. Thermal Science*, 49 (2010), 3, pp. 479-491
- [24] Wang, X., Xu, X., Choi, S. U. S., Thermal Conductivity of Nanoparticle-Fluid Mixture, *Journal of Thermophysics and Heat Transfer*, 13 (1999), 4, pp. 474-480
- [25] Bejan, A., Convection Heat Transfer, John Wiley & Sons, Inc., Hoboken, New Jersey, N. J., USA, 2004
- [26] Maxwell, J., A Treatise on Electricity and Magnetism, 2nd ed., Oxford University Press, Cambridge, UK, 1904
- [27] Patankar, S. V., Numerical Heat Transfer and Fluid Flow, Hemisphere Publishing Corporation, Taylor and Francis Group, New York, USA, 1980
- [28] Oztop, H. F., Dagtekin, I., Mixed Convection in Two Sided Lid-Driven Differentially Heated Square Cavity, *International Journal of Heat and Mass Transfer*, 47 (2004), 8-9, pp. 1761-1769